

1  
2  
3 **Dietary salt promotes cognitive impairment through tau phosphorylation**  
4

5  
6 Giuseppe Faraco<sup>1</sup>  
7

8 Karin Hochrainer<sup>1</sup>  
9

10 Steven G. Segarra<sup>1</sup>  
11

12 Samantha Schaeffer<sup>1</sup>  
13

14 Monica M. Santisteban<sup>1</sup>  
15

16 Ajay Menon<sup>1</sup>  
17

18 Hong Jiang<sup>2</sup>  
19

20 David M. Holtzman<sup>2</sup>  
21

22 Josef Anrather<sup>1</sup>  
23

24 and  
25

26 Costantino Iadecola<sup>1</sup>  
27

28 <sup>1</sup>Feil Family Brain and Mind Research Institute  
29 Weill Cornell Medicine  
30 New York, NY 10065  
31

32 <sup>2</sup>Department of Neurology, Hope Center for Neurological Disorders, Knight Alzheimer's Disease  
33 Research Center,  
34 Washington University  
35 St. Louis, MO 63110  
36  
37  
38  
39  
40  
41

42 Correspondence:

43 Costantino Iadecola, M.D.

44 [coi2001@med.cornell.edu](mailto:coi2001@med.cornell.edu)  
45

46 Giuseppe Faraco, M.D., Ph.D.

47 [gif2004@med.cornell.edu](mailto:gif2004@med.cornell.edu)  
48

49 Feil Family Brain and Mind Research Institute  
50 Weill Cornell Medicine  
51 407 East 61<sup>st</sup> street  
52 New York, NY 10065  
53 Phone: 646-962-8279  
54

1 **Dietary habits and vascular risk factors promote both Alzheimer's disease and cognitive**  
2 **impairment caused by vascular factors<sup>1-3</sup>. Furthermore, accumulation of**  
3 **hyperphosphorylated tau, a microtubule associated protein and a hallmark of Alzheimer's**  
4 **pathology, is also linked to vascular cognitive impairment<sup>4-7</sup>. In mice, a salt-rich diet leads**  
5 **to cognitive dysfunction associated with a nitric oxide deficit in cerebral endothelial cells**  
6 **and cerebral hypoperfusion<sup>8</sup>. Here we report that dietary salt induces tau**  
7 **hyperphosphorylation followed by cognitive dysfunction, effects prevented by restoring**  
8 **endothelial nitric oxide production. The nitric oxide deficiency reduces neuronal calpain**  
9 **nitrosylation resulting in enzyme activation, which, in turn, leads to tau phosphorylation**  
10 **by activating cyclin dependent kinase-5. Salt-induced cognitive impairment is not**  
11 **observed in tau-null mice or in mice treated with anti-tau antibodies, despite persistent**  
12 **cerebral hypoperfusion and neurovascular dysfunction. These findings unveil a causal link**  
13 **between dietary salt, endothelial dysfunction and tau pathology, independent of**  
14 **hemodynamic insufficiency. Avoiding excessive salt intake and maintaining vascular**  
15 **health may help stave off vascular and neurodegenerative pathologies underlying late-life**  
16 **dementia.**

17  
18 Vascular risk factors including excessive salt consumption have long been associated with  
19 cerebrovascular dysfunction and cognitive impairment<sup>1-3</sup>. A diet rich in salt promotes stroke and  
20 dementia independently of hypertension<sup>9-12</sup> and has been linked to the cerebral small vessel  
21 disease underlying vascular cognitive impairment<sup>13,14</sup>, a condition associated with endothelial  
22 dysfunction and reduced cerebral blood (CBF)<sup>15</sup>.

23 Accumulation of the microtubule associated protein tau is a pathological hallmark of  
24 Alzheimer's disease<sup>16</sup>. Excessive tau phosphorylation promotes the formation of insoluble tau  
25 species, thought to mediate neuronal dysfunction and cognitive impairment<sup>17,18</sup>. Tau  
26 hyperphosphorylation and aggregation have increasingly been detected also in vascular brain

1 pathologies both in humans and animal models<sup>4-6</sup>, and have been linked to cognitive dysfunction  
2 in patients with small vessel disease<sup>7</sup>.

3 In mice, a high salt diet (HSD) induces cognitive dysfunction by targeting the cerebral  
4 microvasculature through a gut-initiated adaptive immune response mediated by Th17  
5 lymphocytes<sup>8</sup>. The resulting increase in circulating IL17 leads to inhibition of endothelial nitric  
6 oxide (NO) synthase (eNOS) and reduced NO production in cerebral microvessels, which, in turn,  
7 impairs the endothelial regulation of microvascular flow and lowers cerebral blood flow (CBF) by  
8  $\approx 25\%$ <sup>8</sup>. Remarkably, the increases in CBF evoked by neural activity and blood-brain permeability  
9 are not altered<sup>8</sup>. However, it remains unclear how hypoperfusion, in HSD as in other vascular risk  
10 factors, leads to impaired cognition. The prevailing view is that reduced CBF compromises the  
11 delivery of oxygen and glucose to energy-demanding brain regions involved in cognitive  
12 function<sup>15,19</sup>. But the relatively-small reductions in CBF associated with HSD<sup>8</sup> and vascular  
13 cognitive impairment<sup>20</sup> do not reach the threshold needed to induce sustained cognitive  
14 dysfunction ( $\geq 50\%$  CBF reduction)<sup>21,22</sup>. Thus, vascular factors beyond cerebral perfusion could  
15 also be involved.

16 To address this question, we investigated whether tau contributes to the cognitive  
17 impairment induced by HSD and, if so, whether the effect depends on the associated cerebral  
18 hypoperfusion. First, we established if HSD induces tau phosphorylation. Male C56Bl/6 mice were  
19 placed on a normal diet (ND) or HSD (4 or 8% NaCl), corresponding to a 8-16 fold increase over  
20 the salt content in the regular mouse chow and approaching the highest levels of human salt  
21 consumption<sup>23</sup>. Phosphorylation of selected tau epitopes linked to tau aggregation and neuronal  
22 dysfunction<sup>17</sup> were assessed 4, 8, 12, and 24 weeks later by Western blotting. HSD (8%)  
23 increased p-tau (AT8, RZ3 epitopes) in neocortex and hippocampus without upregulation of total  
24 tau (Tau 46) (Fig. 1A). In the hippocampus, an increase in PHF13 was also observed (Extended  
25 Data Fig. 1A). HSD did not increase tau acetylation, a post translational modification implicated  
26 in the harmful neuronal effects of tau<sup>24</sup> (Extended data Fig. 1A). AT8 and RZ3 were also increased  
27 in neocortex of female mice fed a HSD (Extended data Fig. 1B). AT8 and MC1 immunoreactivity

1 was detected in neuronal cell bodies of the pyriform cortex and other cortical regions, but  
2 neurofibrillary tangles were not observed (Fig. 1B-C; Extended Data Fig. 1C-D). As anticipated,  
3 p-tau (AT8) was abolished by incubation of the sample with lambda protein phosphatase  
4 (Extended Data Fig. 1E). Increased AT8 was also observed in neocortex with a 4% HSD  
5 (Extended Data Fig. 1F), indicating that also lower amounts of dietary salt are sufficient to induce  
6 tau phosphorylation.

7 In neocortex, the increase in AT8 was observed at 4 weeks of HSD and was greatest at  
8 24 weeks, whereas in hippocampus p-tau peaked at 12 weeks and then declined (Fig. 1D and  
9 Extended Data Fig. 1G). An increase in RZ3 was observed at 8 and 12 weeks in neocortex and  
10 at 12 weeks in the hippocampus (Extended Data Fig. 1G). Starting at 12 weeks of HSD, mice  
11 exhibited difficulties in recognizing novel objects and developed a deficit in spatial memory at the  
12 Barnes maze, suggesting impaired cognition (Fig.1E; Extended Data Fig. 2A). Therefore, tau  
13 phosphorylation occurs in parallel with the endothelial NO deficit previously described<sup>8</sup> and is  
14 followed by cognitive deficits. To determine if p-tau is upregulated also in other conditions  
15 associated with endothelial dysfunction, we investigated models of hypertension in which deficits  
16 in endothelial NO and cognitive function are well described<sup>25</sup>. We found an increase in p-tau in  
17 hypertension produced by chronic administration of the pressor peptide angiotensin-II or in  
18 BPH/2J mice with life-long elevations in blood pressure (Extended Data Fig. 2B-C).

19 Tau solubility is a critical determinant of its harmful neuronal effects, and insoluble tau has  
20 been implicated in the neuronal dysfunction driving cognitive impairment<sup>17</sup>. To determine whether  
21 HSD alters tau solubility, tau levels were examined in neocortical and hippocampal lysates by  
22 Western blotting after sequential biochemical extraction in RAB (salt buffer), RIPA (detergent  
23 buffer) or 70% formic acid (FA), containing, respectively, soluble, less soluble and highly insoluble  
24 tau. After 12 weeks of HSD the tau in RIPA and FA fractions increased in neocortex and  
25 hippocampus, consistent with an increase in more insoluble tau (Fig. 1F-G). Since hypothermia  
26 in the setting of hibernation increases p-tau levels without causing cognitive impairment<sup>26</sup>, we  
27 performed a similar analysis in the brain of mice subjected to hypothermia. We found that

1 hypothermia increases p-tau, but, at variance with HSD, does not produce a shift towards more  
2 insoluble species (Extended Data Fig. 2D-E). These observations indicate that HSD leads to tau  
3 phosphorylation and a shift from soluble to insoluble tau.

4 The NO precursor L-arginine counteracts the deficit in endothelial NO induced by HSD<sup>8</sup>  
5 and other conditions associated with endothelial dysfunction<sup>27,28</sup>. Therefore, we asked if L-  
6 arginine would also rescue the p-tau accumulation induced by HSD and, if so, whether the effect  
7 is associated with improved cognition. To this end, mice were given L-arginine in the drinking  
8 water (10gr/L) during the last 4 weeks of the HSD or ND 12 week-treatment. We have previously  
9 demonstrated that L-arginine normalizes resting and stimulated cerebral endothelial NO synthesis  
10 without affecting arterial pressure<sup>8</sup>. L-arginine suppressed p-tau accumulation both in neocortex  
11 (AT8 and RZ3) and hippocampus (AT8) and prevented the cognitive dysfunction induced by HSD  
12 (Fig. 2A-D; Extended Data Fig. 3A).

13 Cdk5 is a major kinase responsible for tau hyperphosphorylation<sup>29</sup>. Cdk5 activity is tightly  
14 regulated by its protein binding partners, including p35<sup>30</sup>. In conditions associated with neuronal  
15 stress, cleavage of p35 into p25 by calpain leads to dysregulated activation of Cdk5 and  
16 hyperphosphorylation of its targets, including tau<sup>31,32</sup>. Since reduced endothelial NO may lead to  
17 tau phosphorylation by activating Cdk5 via p25<sup>33</sup>, we examined if HSD influences calpain and  
18 Cdk5 activity. Calpain 2 is more abundant than calpain 1 in neocortex (Fig. 3A), is located mainly  
19 in neurons (Extended Data Fig. 3B)<sup>34</sup> and colocalizes with Cdk5 (Extended Data Fig. 3C). HSD  
20 did not alter calpain expression (Fig. 3A), but resulted in activation of the enzyme, leading to an  
21 increase in the p25/p35 ratio, in Cdk5 bound to p25/p35 and in Cdk5 catalytic activity (Fig. 3A-C).  
22 Attesting to the involvement of endothelial NO, L-arginine administration prevented the calpain  
23 activation induced by HSD and the resulting increase in the Cdk5/p25/p35 complex and enzyme  
24 activation (Fig. 3D-E). L-arginine did not alter calpain levels (Extended Data Fig. 3D). GSK3 $\beta$  has  
25 also been implicated in tau phosphorylation, but HSD did not increase the activity of this enzyme  
26 in neocortex (Extended Data Fig. 3E). Similarly, HSD did not alter the expression of the prolyl  
27 cis/trans isomerase Pin-1, a regulator of tau dephosphorylation<sup>35</sup> (Extended Data Fig. 3F).

1           Next, we examined the potential mechanisms by which endothelial NO deficiency may  
2 influence calpain activity. Calpain, once activated by  $Ca^{2+}$ , is regulated mainly by its endogenous  
3 inhibitor calpastatin and by nitrosylation by  $NO^{36}$ , which suppress calpain activity<sup>37</sup>. Since HSD  
4 did not reduce calpastatin expression (Extended Data Fig. 3G), we used the biotin switch assay  
5 to investigate the effect of HSD on calpain nitrosylation. Consistent with the observed calpain  
6 activation, we found that HSD reduces calpain nitrosylation (Fig. 3F).

7           The findings thus far suggest that HSD leads to neuronal p-tau accumulation through a  
8 deficit in endothelial NO resulting in denitrosylation and activation of calpain, which, in turn  
9 increases p25 levels resulting in activation of Cdk5. However, HSD also lowers resting CBF and  
10 impairs the ability of endothelial cells to regulate CBF, which could contribute to impair cognition  
11 by reducing the delivery of oxygen and glucose to brain regions involved in cognitive function<sup>19,38</sup>.  
12 Therefore, we examined the relative contribution of p-tau and neurovascular dysfunction to the  
13 cognitive deficits induced by HSD. We reasoned that if tau is critical for the cognitive dysfunction,  
14 then tau-null mice should be protected from the deleterious cognitive effects of HSD despite  
15 sustained cerebral hemodynamic dysfunction. Tau-null mice were placed on ND or HSD and  
16 cerebral endothelial vasomotor function and cognition were assessed 12 weeks later. As  
17 anticipated<sup>39</sup>, the performance of tau-null mice to the novel object recognition test and Barnes  
18 maze was not different from that of WT controls fed a ND (Fig. 4A-C). Tau-null mice on HSD did  
19 not exhibit cognitive impairment, but still exhibited marked endothelial dysfunction, as reflected  
20 by the suppression of the CBF increase induced by bathing the neocortex with acetylcholine (Fig.  
21 4D), a prototypical endothelial response mediated by eNOS-derived  $NO^{38}$ . Therefore, it would  
22 seem that CBF dysregulation is not required for the cognitive dysfunction of HSD. To provide  
23 further evidence in support of this conclusion we treated WT mice with anti-tau antibodies (HJ8.8)  
24 or control IgG (50 mg/kg/week; i.p.) for the last 4 weeks of the 12-week ND or HSD regimen<sup>40</sup>.  
25 Anti-tau antibodies were previously shown to ameliorate cognitive function in a tauopathy mouse  
26 model<sup>40</sup>. In HJ8.8-treated mice, HSD induced a reduction in resting CBF and an attenuation of  
27 the endothelial CBF response to acetylcholine comparable to that observed in HSD-fed mice

1 treated with control IgG (Fig. 4E-F). Despite persistent hypoperfusion and endothelial dysfunction,  
2 anti-tau antibodies ameliorated the cognitive deficit induced by HSD (Fig. 4G). The effect was  
3 associated with a reduction in p-tau in neocortex (AT8) and hippocampus (AT8 and RZ3) (Fig.  
4 4H). As before<sup>8</sup>, HSD did not affect the increases in CBF induced by neural activity (Extended  
5 Data Fig. 4A)

6         These observations, collectively, are consistent with the hypothesis that the reduction in  
7 endothelial NO induced by HSD leads to calpain denitrosylation resulting in activation of the  
8 enzyme. The ensuing increase in p25 activates Cdk5 leading to tau phosphorylation in neurons,  
9 which, in turn, is responsible for the cognitive impairment (Extended Data Fig. 4C). In addition,  
10 the data indicate that the neurovascular dysfunction associated with HSD, also caused by the NO  
11 deficit, is not critical for the cognitive dysfunction. This conclusion is supported by the observations  
12 that the cognitive deficits induced by HSD do not occur in tau-null mice and are ameliorated by  
13 anti-tau antibodies, despite altered endothelium-dependent vasodilatation and reduced CBF.

14         The findings provide novel insights into the mechanisms by which cerebrovascular  
15 dysfunction alters cognition. Although to be confirmed in other cerebrovascular risk factors, the  
16 CBF reduction and suppression of endothelium-dependent vasoreactivity associated with HSD  
17 do not drive cognitive impairment. Whereas the suppression in endothelial NO induced by HSD  
18 is required for the cognitive impairment, the hemodynamic consequences of such NO deficit do  
19 not play a role. Rather, the cognitive dysfunction is dependent on the tau phosphorylation  
20 promoted by the deficit in endothelial NO. Thus, the cerebral hypoperfusion resulting from NO  
21 deficiency seems to be inconsequential to the cognitive deficit. Other aspects of endothelial  
22 function are at play, namely endothelial NO maintaining calpain homeostasis and preventing Cdk5  
23 dysregulation and tau hyperphosphorylation.

24         Our data also provide a previously-unrecognized link between dietary habits, vascular  
25 dysfunction and tau pathology, independently of cerebral hypoperfusion. Such relationship may  
26 play a role in the frequent overlap between vascular and neurogenerative pathologies underlying  
27 late-life dementia<sup>41</sup>. Whereas avoiding excessive salt consumption may help prevent tau

1 pathology, therapeutic efforts to counteract cerebrovascular dysfunction need to go beyond  
2 rescuing cerebral perfusion, and target vascular mediators governing neurovascular interactions  
3 critical for cognitive health.

4

## 5 **MATERIALS AND METHODS**

6 Most of the methods used in this study are well established in the laboratory and have been  
7 described in detail in previous publications<sup>8,25,42</sup>. Here we provide only a brief description.

8

### 9 **Mice**

10 All procedures are approved by the institutional animal care and use committee of Weill Cornell  
11 Medicine (Animal protocol number: 0807-777A). Studies were conducted, according to the  
12 ARRIVE guidelines (<https://www.nc3rs.org.uk/arrive-guidelines>), in the following lines of mice:  
13 C57BL/6 (JAX), B6.129X1-Mapttm1Hnd (Tau<sup>-/-</sup>, JAX, Stock #007251) and Tg(Camk2a-  
14 tTA)1Mmay Fgf<sup>14Tg(tetO-MAPT\*P301L)4510Kha/J</sup> (rTg4510, JAX, Stock#024854), BPH/2J mice (Age: 5  
15 months; JAX, Stock #003005) and BPN/3J mice (Age: 5 months; JAX, Stock #003004). Unless  
16 otherwise indicated, male mice were used.

17

### 18 **High Salt Diet**

19 Male or female mice (8 weeks old) received normal chow (0.5% NaCl) and tap water ad libitum  
20 (normal diet) or sodium-rich chow (4-8% NaCl) and tap water containing 1% NaCl ad libitum  
21 (HSD) for 4 to 24 weeks according to the experiment<sup>8</sup>.

22

### 23 **In vivo treatments**

24 The nitric oxide precursor, L-arginine (10gr/L; Sigma) was administered in the drinking water  
25 starting at 8 weeks of HSD and continuing until 12 weeks. ND and HSD mice were treated (i.p.,  
26 weekly) with 50mg/kg of anti-Tau (HJ8.8) or mouse IgG1 isotype control (Clone MOPC-21;



1 bioXcell) antibodies for the last 4 weeks of the HSD treatment period (12 weeks) prior to  
2 behavioral and cerebrovascular studies.

3

#### 4 **General surgical procedures for CBF studies**

5 Mice were anesthetized with isoflurane (induction, 5%; maintenance, 2%). The trachea was  
6 intubated and mice were artificially ventilated with a mixture of N<sub>2</sub> and O<sub>2</sub>. One of the femoral  
7 arteries was cannulated for recording mean arterial pressure (MAP) and collecting blood samples  
8 for blood gas analysis<sup>43</sup>. Rectal temperature was maintained at 37°C. End tidal CO<sub>2</sub>, monitored  
9 by a CO<sub>2</sub> analyzer (Capstar-100, CWE Inc.), was maintained at 2.6–2.7% to provide a pCO<sub>2</sub> of  
10 30–40 mmHg and a pH of 7.3–7.437. After surgery, isoflurane was discontinued and anesthesia  
11 was maintained with urethane (750 mg/kg, i.p.) and chloralose (50 mg/kg, i.p.). Throughout the  
12 experiment the level of anesthesia was monitored by testing motor responses to tail pinch.

13

#### 14 **Monitoring cerebral blood flow**

15 A small craniotomy (2x2mm) was performed to expose the parietal cortex, the dura was removed,  
16 and the site was superfused with Ringer's solution (37°C; pH 7.3–7.4)<sup>25</sup>. CBF was continuously  
17 monitored at the site of superfusion with a laser-Doppler probe (Perimed) positioned  
18 stereotaxically ≈0.5mm above the cortical surface and connected to a data acquisition system  
19 (PowerLab). CBF values are expressed as percentage increases relative to the resting level.

20

#### 21 **Protocol for CBF experiments**

22 After MAP and blood gases stabilized, CBF responses were recorded<sup>8</sup>. The whisker-barrel cortex  
23 was activated for 60 seconds by stroking the contralateral vibrissae, and the evoked changes in  
24 CBF were recorded. The endothelium-dependent vasodilator acetylcholine (ACh; 100μM; Sigma),  
25 was superfused on the exposed neocortex for 5 minutes and the associated CBF changes were  
26 recorded by laser-Doppler flowmetry.

27

## 1 **Measurement of resting CBF by ASL-MRI**

2 CBF was assessed quantitatively using arterial spin labeling magnetic resonance imaging (ASL-  
3 MRI) as previously described<sup>8</sup>. The ASL images were analyzed by ImageJ and the average CBF  
4 value is reported as mL per 100g of tissue per minute.

## 6 **Osmotic minipumps implantation**

7 Osmotic minipumps containing vehicle (saline) or ANG II (600 ng·kg<sup>-1</sup>·min<sup>-1</sup>) were implanted  
8 subcutaneously under isoflurane anesthesia. Systolic blood pressure was monitored in awake  
9 mice using tail-cuff plethysmography<sup>25</sup>. Forty-two days later, mice were anesthetized and their  
10 brains were collected for assessment of tau phosphorylation.

## 12 **Hypothermia**

13 C57BL/6 mice (12 weeks old) were anesthetized by injection of ketamine/xylazine (100/10  
14 mg/kg). Rectal temperature was continuously monitored and kept at 37°C (normothermia) or 30°C  
15 (hypothermia) using a thermostatically-controlled heating pad. Mice were sacrificed 30 minutes  
16 after anesthesia and their brains were collected and frozen on dry ice. Tissues were kept at -80°C  
17 until processing for immunoblot analysis.

## 19 **Immunoblot analysis**

20 Cortex (≈80-90mg) and hippocampus (≈15mg) isolated from ND and HSD mice were sonicated  
21 in 800 and 600μl of RIPA buffer (50mM Tris-HCl pH 8.0, 150mM NaCl, 0.5% Deoxycholic Acid,  
22 0.1% SDS, 1mM EDTA pH 8.0, 1% IGEPAL CA-630, 1mM Na<sub>3</sub>VO<sub>4</sub>, 20mM NaF and one  
23 tablet/10mL of cOmplete™, EDTA-free Protease Inhibitor Cocktail, Millipore Sigma) and equal  
24 volumes were mixed with SDS sample buffer, boiled, and analyzed on 10% or 10-20% Novex™  
25 WedgeWell™ gels (Thermo Fisher Scientific). Proteins were transferred to PVDF membranes  
26 (Millipore), blocked at room temperature (RT) for 1 hour with 5% milk in TBS, and incubated,  
27 overnight at 4°C, with primary antibodies (see Extended Data Table 1) in 5% BSA in TBS/0.1%

1 Tween-20 (TBST). Membranes were washed in TBST, incubated with goat anti-mouse or rabbit  
2 secondary antibodies conjugated to horseradish peroxidase (Santa Cruz Biotechnology) for 1  
3 hour at RT and protein bands were visualized with Clarity Western ECL Substrate (Bio Rad) on a  
4 Bio Rad ChemiDoc MP Imaging System. Quantification was performed using Image Lab 6.0 (Bio  
5 Rad).

6

### 7 **Heat-stable fractions**

8 After homogenization in cold RIPA buffer and centrifugation, 150µl of the supernatant containing  
9 the proteins was boiled at 100°C for 10 minutes. Samples were cooled on ice for 20 minutes and  
10 then centrifuged at 20,000 g at 4°C for 15 minutes. The supernatant corresponding to the heat  
11 stable (HS) fraction was then harvested. This method is used to isolate proteins resistant to heat  
12 including tau and other microtubule-associated proteins (MAPs). Thus, endogenous  
13 immunoglobulins are precipitated during the boiling process and eliminated from the supernatant.  
14 The proteins were then mixed with equal volumes of SDS sample buffer, boiled, and analyzed on  
15 10% Novex™ WedgeWell™ gels (Thermo Fisher Scientific). Although Tau protein is partially lost  
16 during the boiling process, the HS samples are enriched with Tau (please see Extended Data Fig.  
17 4B). Furthermore, boiling significantly improves specificity of certain antibodies such as AT8, RZ3  
18 or MC1<sup>44</sup>.

19

### 20 **Tau dephosphorylation**

21 After overnight dialysis to remove phosphatase inhibitors, protein samples (40µl) were incubated  
22 with 5µL of 10X NEBuffer for Protein MetalloPhosphatases (PMP), 5µL of 10mM MnCl<sub>2</sub> and 1µl  
23 of Lambda Protein Phosphatase (Lambda PP, New England Biolabs) at 30°C for 3 hours.  
24 Reactions were stopped by addition of SDS sample buffer and boiling for 5 minutes at 100 °C.

25

### 26 **Brain tissue protein extraction**

1 Extraction was performed as described previously<sup>40</sup>. The cortex ( $\approx$ 80-90mg) and the  
2 hippocampus ( $\approx$ 15mg) of each brain were homogenized by sonication in 800 and 300 $\mu$ l of RAB  
3 buffer [100mM MES, 1mM EDTA, 0.5mM MgSO<sub>4</sub>, 750mM NaCl, 20mM NaF, 1mM Na<sub>3</sub>VO<sub>4</sub>,  
4 supplemented by EDTA-free Protease Inhibitor Cocktail, Millipore Sigma], respectively. In brief,  
5 the samples were centrifuged at 50,000g for 20 minutes at 4°C using an Optima MAX-TLA 120.2  
6 Ultracentrifuge (Beckman). The supernatants were collected as RAB soluble fractions and pellets  
7 were resuspended in identical volumes of RIPA buffer [150mM NaCl, 50mM Tris, 0.5%  
8 deoxycholic acid, 1% Triton X-100, 0.5% SDS, 25mM EDTA, pH 8.0, 20mM NaF, 1mM Na<sub>3</sub>VO<sub>4</sub>  
9 supplemented by EDTA-free Protease Inhibitor Cocktail, Millipore Sigma], and centrifuged at  
10 50,000 g for 20 minutes at 4°C. The supernatants were collected as RIPA soluble fractions. The  
11 pellets were sonicated in 70% formic acid (300 $\mu$ l for the cortex and 125 $\mu$ l for the hippocampus),  
12 and centrifuged at 50,000g for 20 minutes at 4°C. The supernatants were collected as 70% formic  
13 acid fractions. All fractions were stored in -80°C until analyzed. For western blotting, an aliquot of  
14 100 $\mu$ l of the formic acid fractions was evaporated in a Savant SpeedVac concentrator at 45°C for  
15 1 hour. The samples were resuspended in 100 $\mu$ l of SDS sample buffer with the addition of 1 $\mu$ l of  
16 10N NaOH, sonicated and then boiled for 5 minutes.

17

## 18 **Immunohistochemistry**

19 After 12 weeks of ND/HSD, mice were anesthetized with intraperitoneal pentobarbital (200  
20 mg/kg), and then perfused transcardially with cold PBS, followed by cold 4% paraformaldehyde  
21 (PFA) in PBS. The brains were removed and immersed first in 4% PFA overnight and then in 70%  
22 ethanol for 3 days. Brains were then embedded in paraffin and cut into 6 $\mu$ m sections using a  
23 microtome. After rehydration and antigen retrieval in preheated citrate buffer (10 $\mu$ M) for 30  
24 minutes, brain sections were immersed in 3% H<sub>2</sub>O<sub>2</sub> and then blocked with 100% Sniper (Biocare  
25 Medical) for 1 hour. After blocking, sections were incubated for 2.5 days at 4°C with the AT8,  
26 MC1, Calpain 2 or Cdk5 antibody (1:250, 1:100, 1:100 and 1:100 in 1:50 Sniper in PBS,  
27 respectively) and thereafter processed for 1 hour with the biotinylated secondary antibody in 1%

1 normal donkey serum PBS (anti-mouse IgG1, Jackson ImmunoResearch) or Cy3 anti-rabbit and  
2 FITC anti-mouse (Jackson ImmunoResearch) for immunofluorescence studies. Reactions were  
3 visualized with the ABC-complex (Vectorlabs) and 3,3-diaminobenzidine. A Nikon light  
4 microscope or a confocal microscope (Leica TCS SP5) was used to visualize the signal  
5 associated with each antibody.

6

### 7 **Thioflavin S Staining**

8 After mounting on slides and post-fixation with 4% PFA in PBS for 10 minutes, coronal brain  
9 sections (40 $\mu$ m) were washed and labeled with 0.05% (wt/vol) thioflavine-S in 50% (vol/vol)  
10 ethanol for 10 minutes as previously described<sup>45</sup>. An epifluorescence microscope (IX83 Inverted  
11 Microscope, Olympus) was used to visualize the FITC signal associated with thioflavine-S.

12

### 13 **Calpain activity**

14 Calpain activity was measured by using a Calpain Activity Assay Kit from AbCam<sup>46,47</sup>. Briefly,  
15 fresh cortex and hippocampus were homogenized in the extraction buffer provided with the kit,  
16 which specifically extracts cytosolic proteins without contaminations of cell membrane and  
17 lysosome proteases and prevents auto-activation of calpain during the extraction procedure. The  
18 fluorometric assay is based on the detection of cleavage of calpain substrate Ac-LLY-AFC. Ac-  
19 LLY-AFC emits blue light ( $\lambda_{max}$  = 400nm); upon cleavage of the substrate by calpain, free AFC  
20 emits a yellow-green fluorescence ( $\lambda_{max}$  = 505nm), which can be quantified using a fluorometer  
21 or a fluorescence plate reader. Specificity of the signal was confirmed by using the calpain  
22 inhibitor Z-LLY-FMK (100-200 $\mu$ M). The activity is expressed as Relative Fluorescent Unit (RFU)  
23 per milligram of protein for each sample.

24

### 25 **p35/p25 and GSK3 $\beta$ immunoprecipitation**

26 Immunoprecipitation was performed with anti-p35p25 (Cell Signaling), anti-GSK3 $\beta$  (Cell  
27 Signaling) or anti-rabbit monoclonal IgG1 isotype control antibody (Santa Cruz Biotechnology).

1 Samples were incubated overnight with the primary antibodies and then with protein-A sepharose  
2 (p35p25) (GE Healthcare Life Sciences) or protein-G Dynabeads (GSK3 $\beta$ ) (Thermo Fisher  
3 Scientific) for 2 hours at 4° C. Precipitates were used for Cdk5 or GSK3 $\beta$  activity measurements.  
4 Immunoprecipitation was confirmed by loading the samples on 10% Tris-glycine SDS  
5 polyacrylamide gels and western blot as described above.

6

### 7 **Detection of S-nitrosylation of calpain 2 with the biotin-switch technique**

8 Detection of S-nitrosylated calpain 2 was performed using the biotin-switch technique, as  
9 previously described<sup>48</sup>. Briefly, samples were sonicated in 800 $\mu$ l of RIPA buffer containing 0.1mM  
10 of neocuproine and, after centrifugation, protein concentrations were measured. Cysteine thiol  
11 groups in 1mg of proteins were blocked with 10% S-methylmethane thiosulfonate (MMTS)  
12 (Sigma). After protein-precipitation with 100% acetone, sodium ascorbate was added to the  
13 sample to convert each S-nitrothiols (SNO) to a free thiol via a transnitrosation reaction to  
14 generate O-nitrosoascorbate. Next, each nascent free thiol (previously an SNO site) was  
15 biotinylated with biotin-HPDP (Pierce). Biotinylated proteins were then pull-down by using avidin  
16 beads and analyzed on 10% Novex™ WedgeWell™ gels (Thermo Fisher Scientific). Before avidin  
17 pulldown, a small fraction of each sample was collected to determine protein “input.” The degree  
18 of pulldown correlates with protein S-nitrosylation of calpain 2 which was detected with an  
19 antibody against the protein (see Extended Data Suppl. Table 1). Nitrosylation of calpain 2 is  
20 expressed as the ratio between the pull-down signal and the input corrected for the  $\beta$ -actin levels.

21

### 22 **Cdk5 and GSK3 $\beta$ activity**

23 Cdk5 activity in brain lysates was determined after pulldown with p25/p35 antibody (Cell  
24 Signaling) from 500 $\mu$ g total protein using a synthetic histone H1 peptide substrate  
25 (PKTPKKAKKL, Enzo Life Sciences). GSK3 $\beta$  activity was determined after pulldown with GSK3 $\beta$   
26 antibody (Cell Signaling) from 100 $\mu$ g total protein using phospho-glycogen synthase peptide-2a  
27 as substrate (Tocris). Phosphorylation reactions were initiated by mixing bead-coupled Cdk5 with

1 40µl reaction buffer containing the following: 50mM HEPES.KOH (pH 7.4), 5mM MgCl<sub>2</sub>, 0.05%  
2 BSA, 50µM substrate, 50µM cold ATP, 1mM dithiothreitol, 1x complete protease inhibitors without  
3 EDTA (Roche Applied Biosciences) and 5 Ci/mmole <sup>γ</sup><sup>32</sup>P-ATP. Companion reactions for every  
4 sample were executed in the presence of the Cdk5 inhibitor ((R)-CR8, Tocris) (10µM) or the  
5 GSK3β inhibitor (CHIR 99021, Tocris) (10µM) to correct for non-specific activity. Reactions were  
6 incubated at 30°C for 30 minutes, after which they were terminated by spotting on P81  
7 phosphocellulose cation exchange chromatography paper. Filters were washed 4 times for 2  
8 minutes in 0.5% phosphoric acid, and the remaining radioactivity was quantified in a scintillation  
9 counter by the Cherenkov method.

10

### 11 **Novel Object Recognition Test**

12 The novel object recognition test (NOR) task was conducted under dim light in a plastic box.  
13 Stimuli consisted of plastic objects that varied in color and shape but had similar size<sup>49,50</sup>. A video  
14 camera mounted on the wall directly above the box was used to record the testing session for off-  
15 line analysis. Mice were acclimated to the testing room and chamber for one day prior to testing.  
16 Twenty-four hours after habituation, mice were placed in the same box in the presence of two  
17 identical sample objects and were allowed to explore for 5 minutes. After an intersession interval  
18 of 1 hour, mice were placed in the same box but one of the two objects was replaced by a novel  
19 object. Mice were allowed to explore for 5 minutes. Exploratory behavior was later assessed  
20 manually by an experimenter blinded to the treatment group. Exploration of an object was defined  
21 as the mouse sniffing the object or touching the object while looking at it. Placing the forepaws on  
22 the objects was considered as exploratory behavior but climbing on the objects was not. A minimal  
23 exploration time for both objects (total exploration time) during the test phase (~5 seconds) was  
24 used. The amount of time taken to explore the novel object was expressed as percentage of the  
25 total exploration time and provides an index of recognition memory<sup>49,50</sup>.

26

### 27 **The Barnes Maze test**

1 The Barnes maze consisted of a circular open surface (90cm in diameter) elevated to 90cm by  
2 four wooden legs<sup>51</sup>. There were 20 circular holes (5cm in diameter) equally spaced around the  
3 perimeter, and positioned 2.5cm from the edge of the maze. No wall and no intra-maze visual  
4 cues were placed around the edge. A wooden plastic escape box (11×6×5cm) was positioned  
5 beneath one of the holes. Two neon lamps and a buzzer were used as aversive stimuli. The Any-  
6 Maze tracking system (Stoelting) was used to record the movement of mice on the maze. Extra-  
7 maze visual cues consisted of objects within the room (table, computer, sink, door, etc.) and the  
8 experimenter. Mice were tested in groups of seven to ten, and between trials they were placed  
9 into cages, which were placed in a dark room adjacent to the test room for the inter-trial interval  
10 (20-30 minutes). No habituation trial was performed. The acquisition phase consisted of 3  
11 consecutive training days with three trials per day with the escape hole located at the same  
12 location across trials and days. On each trial a mouse was placed into a start tube located in the  
13 center of the maze, the start tube was raised, and the buzzer was turned on until the mouse  
14 entered the escape hole. After each trial, mice remained in the escape box for 60 seconds before  
15 being returned to their cage. Between trials the maze floor was cleaned with 10% ethanol in water  
16 to minimize olfactory cues. For each trial mice were given 3 minutes to locate the escape hole,  
17 after which they were guided to the escape hole or placed directly into the escape box if they  
18 failed to enter the escape hole. Four parameters of learning performance were recorded: (1) the  
19 latency to locate (primary latency) and (2) enter the escape hole (total latency), (3) the number of  
20 errors made and (4) the distance traveled before locating the escape hole<sup>51</sup>. When a mouse  
21 dipped its head into a hole that did not provide escape was considered an error. On days 4 and  
22 5, the location of the escape hole was moved 180° from its previous location (reverse learning)  
23 and two trials per day were performed.

24

## 25 **Statistics**

26 Sample size was determined according to power analysis based on previously published work by  
27 our lab on the effects of dietary salt on CBF regulation and cognitive function. On these bases,



1 10-15 mice/group were required in studies involving assessment of cognitive function and  
2 cerebrovascular function<sup>8,25</sup>. Mouse randomization was performed based on the random number  
3 generator function (RANDBETWEEN) in Microsoft Excel software. Analysis of the data was  
4 performed in a blinded fashion and GraphPad Prism (v. 6.0) software was used for statistical  
5 analysis. Intergroup differences were analyzed by unpaired Student's t-test for single comparison  
6 or by one or two-way analysis of variance (Tukey's or Bonferroni's post-hoc analysis) for multiple  
7 comparisons. Data are expressed as mean±SEM and differences are considered statistically  
8 significant for  $p < 0.05$ .

9

#### 10 **Data Availability**

11 All data generated or analyzed during this study are included in this published article (and its  
12 supplementary information files).

13

#### 14 **ACKNOWLEDGEMENTS**

15 We thank Prof. Peter Davies for providing the RZ3, MC1 and PHF1 antibodies. This study was  
16 supported by National Institutes of Health grants R37-NS089323 (CI) and 1R01-NS095441 (CI),  
17 by a grant from the Cure Alzheimer's Fund (GF and CI), and by a Scientist Development Grant  
18 from the American Heart Association (GF). The support from the Feil Family Foundation is  
19 gratefully acknowledged.

20

#### 21 **AUTHOR CONTRIBUTIONS**

22 G.F. performed western blotting experiments, behavioral tests, cerebrovascular studies and  
23 analyzed data. K.H. performed experiments on Cdk5/GSK3 $\beta$  activity and analyzed data. S.G.S.  
24 performed western blotting experiments, behavioral tests and immunohistochemistry. S.S. and  
25 M.M.S. performed experiments on the effects of hypertension on tau. A.M. performed  
26 immunohistochemistry experiments. H.J. and D.M.H. provided the HJ8.8 antibody. J. A

1 supervised the molecular aspects of the study and edited the manuscript. G.F. and C.I. designed  
2 and supervised the entire study and wrote the manuscript.

3  
4 **COMPETING INTERESTS**

5 D.M.H. is listed as an inventor on a patent licensed by Washington University to C2N Diagnostics  
6 and subsequently AbbVie on the therapeutic use of anti-tau antibodies. D.M.H. co-founded and  
7 is on the scientific advisory board of C2N Diagnostics. D.M.H. is on the scientific advisory board  
8 of Denali, Genentech, and Proclara.

9  
10 **REFERENCES**

- 11 1 Scarmeas, N., Anastasiou, C. A. & Yannakoulia, M. Nutrition and prevention of cognitive  
12 impairment. *Lancet Neurol*, doi:10.1016/S1474-4422(18)30338-7 (2018).
- 13 2 van de Rest, O., Berendsen, A. A., Haveman-Nies, A. & de Groot, L. C. Dietary patterns,  
14 cognitive decline, and dementia: a systematic review. *Adv Nutr* **6**, 154-168,  
15 doi:10.3945/an.114.007617 (2015).
- 16 3 Voortman, T. *et al.* Adherence to the 2015 Dutch dietary guidelines and risk of non-  
17 communicable diseases and mortality in the Rotterdam Study. *Eur J Epidemiol* **32**, 993-  
18 1005, doi:10.1007/s10654-017-0295-2 (2017).
- 19 4 Raz, L. *et al.* Hypoxia promotes tau hyperphosphorylation with associated  
20 neuropathology in vascular dysfunction. *Neurobiol Dis*, doi:10.1016/j.nbd.2018.07.009  
21 (2018).
- 22 5 Qiu, L. *et al.* Chronic cerebral hypoperfusion enhances Tau hyperphosphorylation and  
23 reduces autophagy in Alzheimer's disease mice. *Sci Rep* **6**, 23964,  
24 doi:10.1038/srep23964 (2016).
- 25 6 Nation, D. A. *et al.* Pulse pressure in relation to tau-mediated neurodegeneration,  
26 cerebral amyloidosis, and progression to dementia in very old adults. *JAMA Neurol* **72**,  
27 546-553, doi:10.1001/jamaneurol.2014.4477 (2015).
- 28 7 Kim, H. J. *et al.* Assessment of Extent and Role of Tau in Subcortical Vascular Cognitive  
29 Impairment Using 18F-AV1451 Positron Emission Tomography Imaging. *JAMA Neurol*  
30 **75**, 999-1007, doi:10.1001/jamaneurol.2018.0975 (2018).
- 31 8 Faraco, G. *et al.* Dietary salt promotes neurovascular and cognitive dysfunction through  
32 a gut-initiated TH17 response. *Nat Neurosci* **21**, 240-249, doi:10.1038/s41593-017-  
33 0059-z (2018).
- 34 9 Farquhar, W. B., Edwards, D. G., Jurkowitz, C. T. & Weintraub, W. S. Dietary sodium  
35 and health: more than just blood pressure. *J Am Coll Cardiol* **65**, 1042-1050,  
36 doi:10.1016/j.jacc.2014.12.039 (2015).
- 37 10 Strazzullo, P., D'Elia, L., Kandala, N. B. & Cappuccio, F. P. Salt intake, stroke, and  
38 cardiovascular disease: meta-analysis of prospective studies. *BMJ* **339**, b4567,  
39 doi:10.1136/bmj.b4567 (2009).
- 40 11 Fiocco, A. J. *et al.* Sodium intake and physical activity impact cognitive maintenance in  
41 older adults: the NuAge Study. *Neurobiol Aging* **33**, 829 e821-828,  
42 doi:10.1016/j.neurobiolaging.2011.07.004 (2012).
- 43 12 Gardener, H., Rundek, T., Wright, C. B., Elkind, M. S. & Sacco, R. L. Dietary sodium and  
44 risk of stroke in the Northern Manhattan study. *Stroke* **43**, 1200-1205,  
45 doi:10.1161/STROKEAHA.111.641043 (2012).

- 1 13 Makin, S. D. J. *et al.* Small Vessel Disease and Dietary Salt Intake: Cross-Sectional  
2 Study and Systematic Review. *J Stroke Cerebrovasc Dis* **26**, 3020-3028,  
3 doi:10.1016/j.jstrokecerebrovasdis.2017.08.004 (2017).
- 4 14 Heye, A. K. *et al.* Blood pressure and sodium: Association with MRI markers in cerebral  
5 small vessel disease. *J Cereb Blood Flow Metab* **36**, 264-274,  
6 doi:10.1038/jcbfm.2015.64 (2016).
- 7 15 Iadecola, C. The pathobiology of vascular dementia. *Neuron* **80**, 844-866,  
8 doi:10.1016/j.neuron.2013.10.008 (2013).
- 9 16 Scheltens, P. *et al.* Alzheimer's disease. *Lancet* **388**, 505-517, doi:10.1016/S0140-  
10 6736(15)01124-1 (2016).
- 11 17 Wang, Y. & Mandelkow, E. Tau in physiology and pathology. *Nat Rev Neurosci* **17**, 5-21,  
12 doi:10.1038/nrn.2015.1 (2016).
- 13 18 Despres, C. *et al.* Identification of the Tau phosphorylation pattern that drives its  
14 aggregation. *Proc Natl Acad Sci U S A* **114**, 9080-9085, doi:10.1073/pnas.1708448114  
15 (2017).
- 16 19 Sweeney, M. D., Kisler, K., Montagne, A., Toga, A. W. & Zlokovic, B. V. The role of brain  
17 vasculature in neurodegenerative disorders. *Nat Neurosci* **21**, 1318-1331,  
18 doi:10.1038/s41593-018-0234-x (2018).
- 19 20 Shi, Y. *et al.* Cerebral blood flow in small vessel disease: A systematic review and meta-  
20 analysis. *J Cereb Blood Flow Metab* **36**, 1653-1667, doi:10.1177/0271678X16662891  
21 (2016).
- 22 21 Tatemichi, T. K., Desmond, D. W., Prohovnik, I. & Eidelberg, D. Dementia associated  
23 with bilateral carotid occlusions: neuropsychological and haemodynamic course after  
24 extracranial to intracranial bypass surgery. *J Neurol Neurosurg Psychiatry* **58**, 633-636  
25 (1995).
- 26 22 Marshall, R. S. *et al.* Cerebral hemodynamics and cognitive impairment: baseline data  
27 from the RECON trial. *Neurology* **78**, 250-255, doi:10.1212/WNL.0b013e31824365d3  
28 (2012).
- 29 23 Powles, J. *et al.* Global, regional and national sodium intakes in 1990 and 2010: a  
30 systematic analysis of 24 h urinary sodium excretion and dietary surveys worldwide.  
31 *BMJ Open* **3**, e003733, doi:10.1136/bmjopen-2013-003733 (2013).
- 32 24 Min, S. W. *et al.* Critical role of acetylation in tau-mediated neurodegeneration and  
33 cognitive deficits. *Nat Med* **21**, 1154-1162, doi:10.1038/nm.3951 (2015).
- 34 25 Faraco, G. *et al.* Perivascular macrophages mediate the neurovascular and cognitive  
35 dysfunction associated with hypertension. *J Clin Invest* **126**, 4674-4689,  
36 doi:10.1172/JCI86950 (2016).
- 37 26 Arendt, T., Stieler, J. T. & Holzer, M. Tau and tauopathies. *Brain Res Bull* **126**, 238-292,  
38 doi:10.1016/j.brainresbull.2016.08.018 (2016).
- 39 27 Rosenblum, W. I., Nelson, G. H. & Shimizu, T. L-arginine suffusion restores response to  
40 acetylcholine in brain arterioles with damaged endothelium. *Am J Physiol* **262**, H961-  
41 964, doi:10.1152/ajpheart.1992.262.4.H961 (1992).
- 42 28 Yamada, M. *et al.* Endothelial nitric oxide synthase-dependent cerebral blood flow  
43 augmentation by L-arginine after chronic statin treatment. *J Cereb Blood Flow Metab* **20**,  
44 709-717, doi:10.1097/00004647-200004000-00008 (2000).
- 45 29 Kimura, T., Ishiguro, K. & Hisanaga, S. Physiological and pathological phosphorylation  
46 of tau by Cdk5. *Front Mol Neurosci* **7**, 65, doi:10.3389/fnmol.2014.00065 (2014).
- 47 30 Tsai, L. H., Delalle, I., Caviness, V. S., Jr., Chae, T. & Harlow, E. p35 is a neural-specific  
48 regulatory subunit of cyclin-dependent kinase 5. *Nature* **371**, 419-423,  
49 doi:10.1038/371419a0 (1994).
- 50 31 Lee, M. S. *et al.* Neurotoxicity induces cleavage of p35 to p25 by calpain. *Nature* **405**,  
51 360-364, doi:10.1038/35012636 (2000).
- 52 32 Patrick, G. N. *et al.* Conversion of p35 to p25 deregulates Cdk5 activity and promotes  
53 neurodegeneration. *Nature* **402**, 615-622, doi:10.1038/45159 (1999).

- 1 33 Austin, S. A. & Katusic, Z. S. Loss of Endothelial Nitric Oxide Synthase Promotes p25  
2 Generation and Tau Phosphorylation in a Murine Model of Alzheimer's Disease. *Circ*  
3 *Res* **119**, 1128-1134, doi:10.1161/CIRCRESAHA.116.309686 (2016).
- 4 34 Adamec, E., Mohan, P., Vonsattel, J. P. & Nixon, R. A. Calpain activation in  
5 neurodegenerative diseases: confocal immunofluorescence study with antibodies  
6 specifically recognizing the active form of calpain 2. *Acta Neuropathol* **104**, 92-104,  
7 doi:10.1007/s00401-002-0528-6 (2002).
- 8 35 Kimura, T. *et al.* Isomerase Pin1 stimulates dephosphorylation of tau protein at cyclin-  
9 dependent kinase (Cdk5)-dependent Alzheimer phosphorylation sites. *J Biol Chem* **288**,  
10 7968-7977, doi:10.1074/jbc.M112.433326 (2013).
- 11 36 Ono, Y., Saido, T. C. & Sorimachi, H. Calpain research for drug discovery: challenges  
12 and potential. *Nat Rev Drug Discov* **15**, 854-876, doi:10.1038/nrd.2016.212 (2016).
- 13 37 Etwebi, Z., Landesberg, G., Preston, K., Eguchi, S. & Scalia, R. Mechanistic Role of the  
14 Calcium-Dependent Protease Calpain in the Endothelial Dysfunction Induced by MPO  
15 (Myeloperoxidase). *Hypertension* **71**, 761-770,  
16 doi:10.1161/HYPERTENSIONAHA.117.10305 (2018).
- 17 38 Iadecola, C. The Neurovascular Unit Coming of Age: A Journey through Neurovascular  
18 Coupling in Health and Disease. *Neuron* **96**, 17-42, doi:10.1016/j.neuron.2017.07.030  
19 (2017).
- 20 39 Ahmed, T. *et al.* Cognition and hippocampal synaptic plasticity in mice with a  
21 homozygous tau deletion. *Neurobiol Aging* **35**, 2474-2478,  
22 doi:10.1016/j.neurobiolaging.2014.05.005 (2014).
- 23 40 Yanamandra, K. *et al.* Anti-tau antibodies that block tau aggregate seeding in vitro  
24 markedly decrease pathology and improve cognition in vivo. *Neuron* **80**, 402-414,  
25 doi:10.1016/j.neuron.2013.07.046 (2013).
- 26 41 Power, M. C. *et al.* Combined neuropathological pathways account for age-related risk of  
27 dementia. *Ann Neurol* **84**, 10-22, doi:10.1002/ana.25246 (2018).
- 28 42 Hochrainer, K. *et al.* The ubiquitin ligase HERC3 attenuates NF-kappaB-dependent  
29 transcription independently of its enzymatic activity by delivering the RelA subunit for  
30 degradation. *Nucleic Acids Res* **43**, 9889-9904, doi:10.1093/nar/gkv1064 (2015).
- 31 43 Faraco, G. *et al.* Circulating endothelin-1 alters critical mechanisms regulating cerebral  
32 microcirculation. *Hypertension* **62**, 759-766,  
33 doi:10.1161/HYPERTENSIONAHA.113.01761 (2013).
- 34 44 Petry, F. R. *et al.* Specificity of anti-tau antibodies when analyzing mice models of  
35 Alzheimer's disease: problems and solutions. *PLoS One* **9**, e94251,  
36 doi:10.1371/journal.pone.0094251 (2014).
- 37 45 Faraco, G. *et al.* Hypertension enhances Abeta-induced neurovascular dysfunction,  
38 promotes beta-secretase activity, and leads to amyloidogenic processing of APP. *J*  
39 *Cereb Blood Flow Metab* **36**, 241-252, doi:10.1038/jcbfm.2015.79 (2016).
- 40 46 Voit, A. *et al.* Reducing sarcolipin expression mitigates Duchenne muscular dystrophy  
41 and associated cardiomyopathy in mice. *Nat Commun* **8**, 1068, doi:10.1038/s41467-017-  
42 01146-7 (2017).
- 43 47 Liu, W. *et al.* Metabolic stress-induced cardiomyopathy is caused by mitochondrial  
44 dysfunction due to attenuated Erk5 signaling. *Nat Commun* **8**, 494, doi:10.1038/s41467-  
45 017-00664-8 (2017).
- 46 48 Forrester, M. T., Foster, M. W., Benhar, M. & Stamler, J. S. Detection of protein S-  
47 nitrosylation with the biotin-switch technique. *Free Radic Biol Med* **46**, 119-126,  
48 doi:10.1016/j.freeradbiomed.2008.09.034 (2009).
- 49 49 Cohen, S. J. & Stackman, R. W., Jr. Assessing rodent hippocampal involvement in the  
50 novel object recognition task. A review. *Behav Brain Res* **285**, 105-117,  
51 doi:10.1016/j.bbr.2014.08.002 (2015).
- 52 50 Grayson, B. *et al.* Assessment of disease-related cognitive impairments using the novel  
53 object recognition (NOR) task in rodents. *Behav Brain Res* **285**, 176-193,  
54 doi:10.1016/j.bbr.2014.10.025 (2015).

1 51 O'Leary, T. P. & Brown, R. E. Optimization of apparatus design and behavioral  
2 measures for the assessment of visuo-spatial learning and memory of mice on the  
3 Barnes maze. *Learn Mem* **20**, 85-96, doi:10.1101/lm.028076.112 (2013).  
4

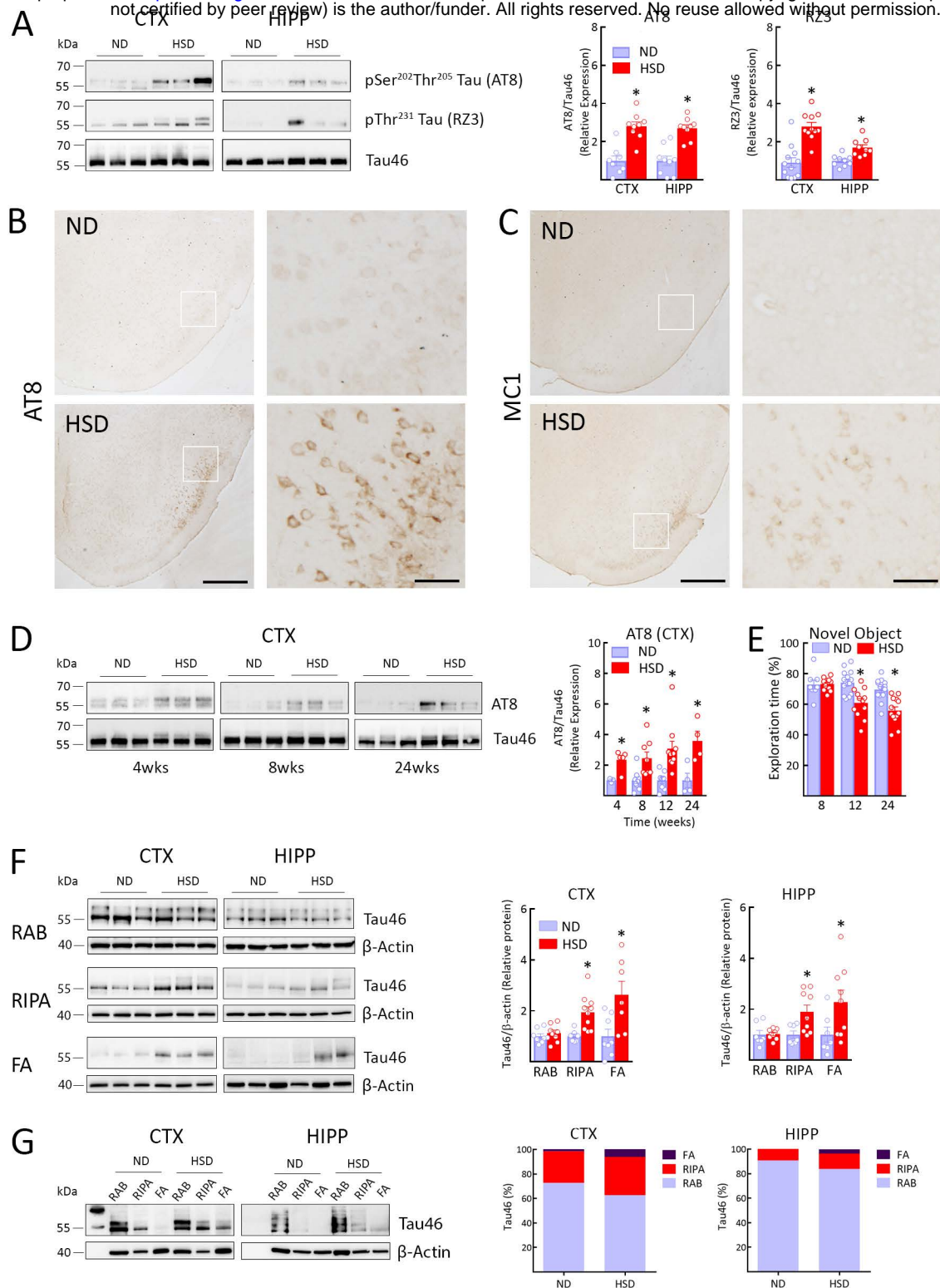


**Figure 1**

**HSD increases tau phosphorylation and insoluble tau. A-B:** HSD (NaCl 8%) increases tau phosphorylation on Ser<sup>202</sup>Thr<sup>205</sup> (AT8) and Thr<sup>231</sup> (RZ3) both in neocortex and hippocampus. (CTX: AT8, ND/HSD n=8/9, \*p=0.0003 vs ND; RZ3, ND/HSD n=12/11, \*p<0.0001 vs ND; HIPP: AT8, ND/HSD n=9/9, \*p=0.0005 vs ND; RZ3, ND/HSD n=9/9, \*p=0.0008 vs ND, two-tailed unpaired t-test). **C:** HSD increases AT8 and MC1 immunoreactivity in neuronal cell bodies of the piriform cortex (size bar=500 μm; 100 μm in inset). **D:** Time course of the increase in AT8 induced by HSD in the neocortex. The increase is observed at 4 weeks and is greatest at 24 weeks of HSD (AT8, 4 weeks: ND/HSD n=3/5, \*p=0.0357 vs ND 4wks; 8 weeks: ND/HSD n=9/8, \*p=0.0016 vs ND 8wks; 24 weeks: ND/HSD n=4/4, \*p=0.0286 vs ND 24wks, two-tailed unpaired t-test). **E:** HSD induces deficits in recognition memory assessed by the novel object test, first observed at 12 weeks (Diet: \*p<0.0001, Time: \*p=0.0002; 8 weeks: ND/HSD n=8/11; 12 weeks: ND/HSD n=16/12; 24 weeks: ND/HSD n=14/13 mice/group, two-way ANOVA and Tukey's test). **F:** Extraction of total tau in RAB, RIPA and 70% FA buffer in neocortex and hippocampus. HSD increases levels of tau extracted in RIPA and FA after 12 weeks of treatment indicating increased insolubility (CTX: RIPA, ND/HSD n=7/10, \*p=0.0032 vs ND RIPA; FA, ND/HSD n=8/7, \*p=0.0146 vs ND FA; HIPP: RIPA, ND/HSD n=7/9, \*p=0.0186 vs ND RIPA; FA, ND/HSD n=7/9, \*p=0.0494 vs ND FA, two-tailed unpaired t-test). **G:** Fractionation of total tau in RAB, RIPA, or 70% FA. HSD shifts tau from the more soluble RAB fraction to the less soluble RIPA and FA fractions (CTX: ND/HSD n=9/8, RAB, p=0.4234 vs ND, RIPA, p=0.5414 vs ND, FA, \*p<0.0325 vs ND; HIPP: ND/HSD n=5/6, RAB, p=0.2468 vs ND, RIPA, p=0.3290 vs ND, FA, \*p<0.0152 vs ND, two-tailed unpaired t-test). Immunoblots in **A**, **D**, **F** and **G** are cropped. Full gel pictures for immunoblots are shown in Extended Data Fig.5 and 6. Data are expressed as mean±SEM.

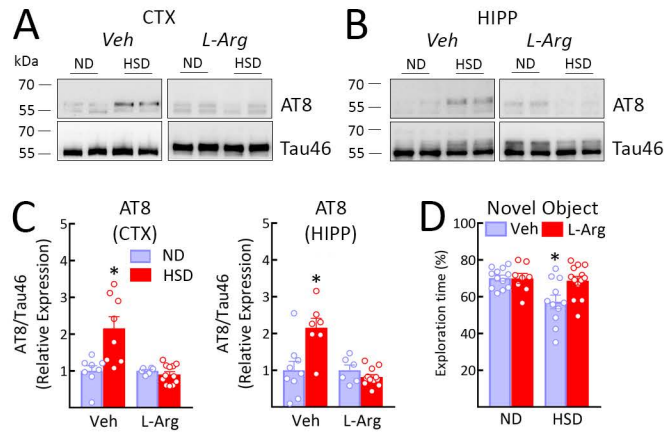


**Figure 2**

**The NO precursor L-arginine prevents the increase in p-tau induced by HSD. A-C:** Administration of L-arginine (10 g/L in drinking water), starting at week 8 of HSD and continued through week 12, suppresses AT8 accumulation in both neocortex and hippocampus (CTX: Vehicle, ND/HSD n=8/8, Diet: \*p=0.0060, Treatment: \*p=0.0015; HIPP: Vehicle, ND/HSD n=9/7, Diet: \*p=0.0145, Treatment: \*p=0.0011, two-way ANOVA and Bonferroni's test). **D:** L-arginine treatment improves the cognitive deficits induced by HSD (Veh – ND/HSD n=12/10, L-Arg – ND/HSD n=6/11; Diet: \*p=0.0156, Treatment: \*p=0.0406, two-way ANOVA and Tukey's test). Immunoblots in **A** and **B** are cropped. Full gel pictures for immunoblots are shown in Extended Data Fig.7. Data are expressed as mean±SEM.

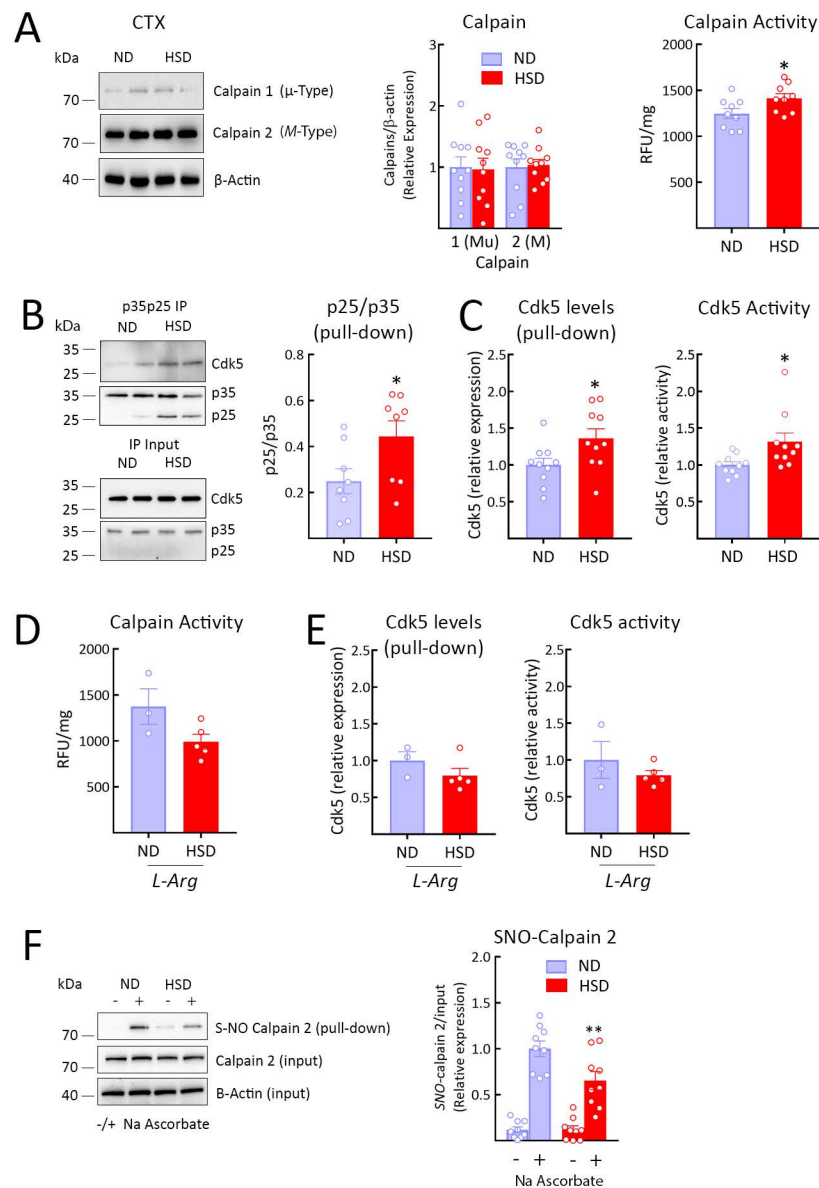


**Figure 3**  
**HSD induces activation of calpain and Cdk5, an effect associated with calpain denitrosylation.** **A:** HSD did not alter calpain 1 or 2 expression (ND/HSD, n=10), but increased enzyme activity (ND/HSD n=9/9, \*p=0.0314 vs ND, two-tailed unpaired t-test). **B:** Consistent with calpain activation, HSD increases the cleavage of p35 into p25 (ND/HSD n=8/8, \*p=0.0379 vs ND, two-tailed unpaired t-test). **C:** HSD increases the levels of Cdk5 bound to p35p25 (ND/HSD n=10/10, \*p=0.0232 vs ND, two-tailed unpaired t-test) and Cdk5 activity (ND/HSD n=10/10, \*p=0.0115 vs ND, two-tailed unpaired t-test). **D-E:** L-arginine administration counteracts the increase in calpain and Cdk5 activity induced by HSD (ND/HSD n=3/5). **F:** Nitrosylation of calpain 2, the predominant brain isoform of the enzyme (see **A**), is reduced in HSD mice (ND/HSD n=9/9, Diet: \*p=0.0189; Treatment: \*p<0.0001, two-way ANOVA and Tukey's test). Nitrosylation was assessed by the biotin switch assay. Immunoblots in **A**, **B** and **F** are cropped. Full gel pictures for immunoblots are shown in Extended Data Fig.8. Data are expressed as mean $\pm$ SEM.



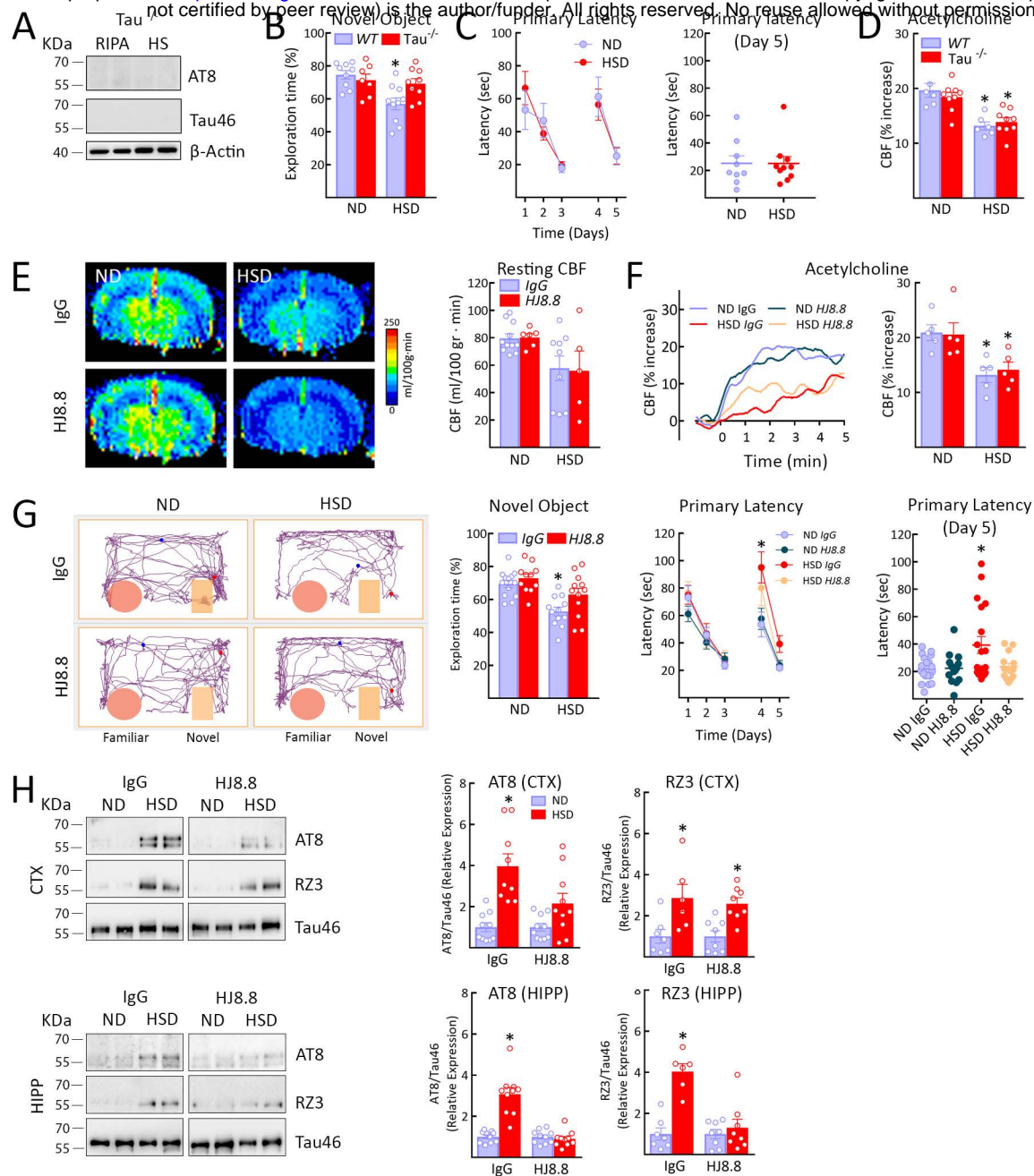


**Figure 4**

**HSD-induced cognitive dysfunction is not observed in tau<sup>-/-</sup> mice and prevented by tau antibodies despite cerebrovascular insufficiency.**

**A:** AT8 and Tau46 are absent in tau<sup>-/-</sup> mice in both the RIPA and heat-stable RIPA fractions. **B-C:** HSD does not alter cognitive function in tau<sup>-/-</sup> mice, assessed by the novel object recognition test (WT: ND/HSD n=9/10; Tau<sup>-/-</sup>: ND/HSD n=7/9; Diet: \*p=0.0055, Genotype: p=0.1827, two-way ANOVA and Tukey's test) or the Barnes maze (ND/HSD n=9/10, Diet: p=0.9348, Time: \*p<0.0001, Two-way ANOVA and Tukey's test). **D:** Despite improved cognition, the CBF increase produced by neocortical application of acetylcholine in anesthetized mice equipped with a cranial window, a response mediated by eNOS-derived NO, is still reduced in tau<sup>-/-</sup> mice (ND/HSD WT, n=6/6, Tau<sup>-/-</sup>, n=9/9; Diet: \*p<0.0001, Genotype: p=0.7920, Two-way ANOVA and Tukey's test). CBF was measured by laser-Doppler flowmetry. **E:** Systemic administration of anti-tau antibodies (HJ8.8, 50mg/Kg/week i.p.) does not rescue the reduction in resting CBF induced by HSD, assessed by ASL-MRI (IgG: ND/HSD n=11/9; HJ8.8: ND/HSD n=6/5; Diet: \*p=0.0061, Treatment: p=0.9367, two-way ANOVA and Tukey's test). **F:** Similarly, HJ8.8 administration does not prevent the attenuation of the CBF response to ACh induced by HSD (IgG: ND/HSD n=5/5; HJ8.8: ND/HSD n=5/5; Diet: \*p=0.0005, Treatment: p=0.8516, two-way ANOVA and Tukey's test). **G:** HJ8.8 administration ameliorates the cognitive dysfunction induced by HSD both at the novel object test (IgG: ND/HSD n=13/12; HJ8.8: ND/HSD n=11/12; Diet: \*p<0.0001, Treatment: \*p=0.0231, two-way ANOVA and Tukey's test) and the Barnes maze (Primary Latency - IgG: ND/HSD n=19/19; HJ8.8: ND/HSD n=13/14; Time: \*p<0.0061, Diet: \*p=0.0317, repeated-measures two-way ANOVA and Tukey's test; Primary Latency - Day 5 - IgG: ND/HSD n=19/19; HJ8.8: ND/HSD n=13/14; Diet: \*p=0.0320, Treatment: p=0.0756, two-way ANOVA and Tukey's test). **H:** HJ8.8 administration reduces AT8 levels in both neocortex and hippocampus (AT8, CTX - IgG: ND/HSD n=10/9; HJ8.8: ND/HSD n=10/10; Diet: \*p<0.0001, Treatment: \*p=0.0313; AT8 - HIPP - IgG: ND/HSD n=10/10; HJ8.8: ND/HSD n=10/10; Diet: \*p<0.0001, Treatment: \*p<0.0001, two-way ANOVA and Bonferroni's test) and RZ3 levels in the hippocampus but not neocortex (RZ3, CTX - IgG: ND/HSD n=7/7; HJ8.8: ND/HSD n=8/8; Diet: \*p=0.0005, Treatment: p=0.9586, RZ3 - HIPP - IgG: ND/HSD n=7/6; HJ8.8: ND/HSD n=8/8; Diet: \*p<0.0001, Treatment: \*p=0.0004, two-way ANOVA and Bonferroni's test). Immunoblots in **A** and **H** are cropped. Full gel pictures for immunoblots are shown in Extended Data Fig.9. Data are expressed as mean±SEM.